Mat. Res. Soc. Symp. Proc. Vol. 724 © 2002 Materials Research Society

Nanoscale Patterning of Antigen on Silicon Substrate to Examine Mast Cell Activation

Reid N. Orth[1*], Min Wu[2*], Theodore G. Clark[3], David A. Holowka[2], Barbara A. Baird[2], and Harold G. Craighead[1]
[1]School of Applied and Engineering Physics, [2]Department of Chemistry and Chemical Biology, Cornell University, [3]Department of Microbiology and Immunology Ithaca, NY 14853

ABSTRACT

Rat Basophilic Leukemia (RBL) cells are immobilized and stimulated on micro- and nanometer scale patterns of supported lipid bilayers. The patterns are realized as the photolithographically patterned polymer is mechanically peeled away in one contiguous piece in solution. The 0.36 μm^2 to 4,489 μm^2 patches can contain both fluorescent lipids and lipid-linked antigen and provide a synthetic biological substrate for analysis of cell surface receptor-mediated events. 100-nm unilamellar lipid vesicles spread to form a supported lipid bilayer on a thermally oxidized silicon surface as confirmed by fluorescence recovery after photobleaching (FRAP). Aggregation of fluorescently labeled receptors is observed as their coincidence with the patterned antigen. Cell morphology is analyzed with scanning electron microscopy (SEM). Thus, a novel method has been developed for patterning antigen, capturing and immobilizing cells via specific receptors, and spatially controlling antigenic stimulus on the nanoscale.

INTRODUCTION

Dinitrophenyl-conjugated lipids have been patterned on the micro- and nanometer scale to spatially control the stimulation of specific immunoreceptors on RBL mast cells. This work was motivated by previous research to elucidate the cascade of events from the initial receptor ligand interaction through cellular activation. Typically, many membrane-bound molecules work collectively to achieve specific cell-cell and cell-substrate recognition. The immunological synapse formation between antigen receptors on T cells (TCR) and antigen presenting cells is an example of the complex interaction initiating T cell activation in many immune responses [1].

IgE receptors (IgE-FcεRI) on mast cells are structurally and functionally similar to TCR and they are mainly involved in the allergic immune response and related inflammatory diseases. IgE are soluble, Y-shaped antibodies with binding sites for antigen in each of two segments. The third segment binds tightly to FcεRI on the mast cell surface, thereby becoming part of the receptor and effectively sensitizing the cell to the specific antigen. Cross-linking of IgE-FcεRI by bi- or multivalent antigens initiates transmembrane signaling which leads to exocytosis of secretory granules containing histamine and other inflammatory mediators. Mast cells are long-term residents of vascularized tissues and have specific roles in acute, 'late phase' and chronic aspects of adaptive or pathological IgE-associated acquired immune responses [2].

Recent research on immunoreceptor signaling has begun to focus on the initial stages involving specialized membrane domains, commonly called lipid rafts. In the mast cell system, for example, coalesced lipid rafts facilitate functional coupling of antigen-crosslinked IgE-FcεRI with the first signaling component on the cytoplasmic side of the membrane, the Lyn tyrosine kinase. Similar observations have been made for T cells and B cells operating in other immune responses [3]. Assembly of the signaling complex of enzymes and scaffolding proteins occurs with localization provided by the plasma membrane that is organized around the cross-linked

* Co first authors

receptors. Interplay between these domains and the actin-cytoskeleton affects the localization and thereby the manner in which signaling proceeds. Such structural localization allows the cell to respond rapidly to a variety of stimuli with a limited number of targeted signaling components. Although this view is supported with a large accumulation of data, important details of the localized assembly remain to be elucidated. Systematic examination requires spatial and ultimately temporal control over the initial stimuli that can be exerted with appropriately engineered molecules and surfaces.

Microfabrication advances have enabled subcellular biomaterials patterning. These methods have enabled enzymes, antibodies, and nucleic acids to be spatially distributed on silicon, glass, and plastic substrates [4]. Recent lipid patterning techniques using microfabrication offer new methods for analyzing lipid characteristics including the formation, stability, and sensitivity of lipid bilayers on solid substrates [5-7]. Microcontact printing [8,9] has been used to study supported lipid bilayer lateral diffusion [10], mobility within confined barriers [11], and formation of concentration gradients during electrophoresis [12]. Barriers to lipid bilayers were formed on silicon with 10-nm thick gold corrals [13] and mechanical scratches [14]. Cell studies involving micropatterned biomaterials on solid substrates include microcontact printing anti-*E.coli* O157:H7 IgG to capture *E.coli* O157:H7 cells from solution [15], patterning neuronal cells using light-assisted functionalized photoresists [16], and culturing differentiated B104 neuroblastoma cells on four substrates to determine the preferred support substrate [17].

This paper presents a method for spatially patterning an antigenized (haptenated), supported lipid bilayer at sub-micron resolution for mast cell immobilization and activation leading to degranulation. This provides a system to study localized initiation of signal transduction that occurs in mast cells and is a model for the immunological synapse that occurs between T cells and antigen presenting cells. By these means cell surface receptors can be clustered by mobile, specific antigen at natural length scales in the micron and submicron range. Moreover, the size of the patch and the density of the antigen can be systemically tested for functional effects. The patterned, antigen rich surface is created using a polymer lift-off method [18,19]. In this method, the Parylene C, di-para-xylylene, dimer is conformally vapor polymer deposited and photoresist is spun over the thermally oxidized silicon substrate (Figure 1A). Conventional photolithography and reactive ion etching (RIE) pattern the polymer (Figure 1B). Lipid vesicles are applied (Figure 1C). Parylene is removed with a one-step mechanical lift-off (Figure 1D) leaving patterned supported lipid bilayers. RBL cells are sensitized with Alexa-488 labeled IgE

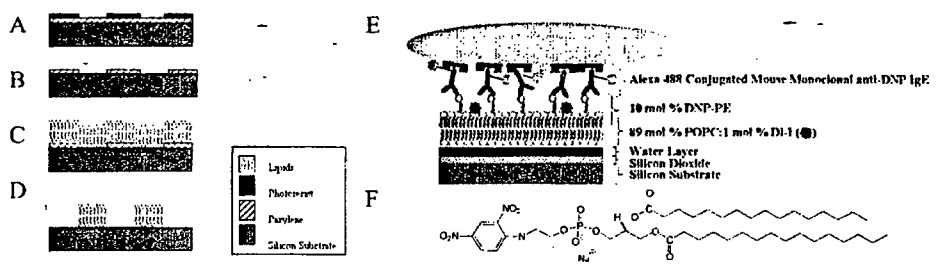

Figure. 1. Fabrication process flow schematic [19]. (A) Photolithography. (B) Reactive ion etching. (C) POPC lipid immobilization. (D) Peeling of Parylene. (E) Schematic of the lipid pattern illustrated in figures 2A and 2B. (F) Dinitrophenyl-phosphoethanolamine structure [20].

and subsequently applied to the hapten-patterned substrate. Confocal and epifluorescence microscopy allow the cell morphology and surface aggregation of IgE-FcεRI with respect to the pattern features to be visualized. SEM imaging provides high-resolution morphological images.

EXPERIMENTAL DETAILS

Reagents. Milli-Q water (18.2 Mohm-cm) was used for rinsing. The OCG_OiR 897-12i photoresist was developed in Microposit MIF 300 (Shipley, Marlboro, MA). N-[2-Hydroxyethyl]piperazine-N'-[2-ethanesulfonic acid]) (HEPES), sodium chloride (NaCl), and phosphate buffered saline (PBS) (Aldrich, Milwaukee, WI) formed the buffer solution.

Silicon Wafer Preparation and Parylene Deposition. 3-inch <1-0-0> N/phos type wafers (Silicon Qwest, Int'l, Santa Clara, CA) were cleaned in base and acid baths to remove surface contaminants and baked at 1100°C for 50 minutes in a wet oxide furnace to grow a 500-nm thermal oxide layer. A pinhole-free conformal layer of Parylene C was deposited using the PDS-2010 Labcoater 2 Parylene deposition system (Specialty Coating Systems, Indianapolis, IN). 1.5 g of Parylene dimer was used to deposit a 1-μm thick Parylene film on 5 3-inch silicon wafers.

Photolithography. 1.5 μm of photoresist was applied to the Parylene-coated silicon wafers and patterned using standard photolithographic techniques. The samples were subjected to an oxygen-based RIE etch, rinsed with acetone and isopropyl alcohol, and dried with a nitrogen gas.

Lipid Preparation. The lipids used include Dinitrophenyl-Phosphoethanolamine (DNP-PE), Di-I-conjugated Dioleoylephosphatidylethanolamine (Di-I-DPPC), and Di-I-conjugated 1-Palmatoyl-2-*SN*-Glycero-3-Phosphocholine ((Di-I-POPC) (Avanti Polar Lipids, Alabaster, Alabama). The POPC:Di-I:DNP (99:1 molar ratio) solution was prepared in chloroform. 5 μmoles of total lipid was transferred to 13x100 mm glass test tubes, dried with nitrogen gas and placed under a 10^{-5} torr vacuum. The solution was rehydrated to a final lipid content of 2 mM using 150 mM NaCl, 10 mM HEPES, pH 7.4. The solutions were vortexed and subjected to 10 freeze-thaw cycles (liquid nitrogen/room temperature water). The vesicle solution was extruded 10 times with a high pressure 10 mL Thermobarrel Extruder (Northern Lipids, Vancouver, British Columbia) as described by Mayer [21] using two stacked 0.1 μm Nucleopore polycarbonate filters (Whatman, Inc., Clifton, NJ) to create 100 nm unilamellar lipid vesicles.

Lipid Application. 10 μl of a 2 mM lipid solution were bath-applied onto the Parylene-patterned polymer substrate. After a 5-minute lipid application, the sample was immersed in water (18-MΩ-cm). The Parylene was mechanically peeled from the surface and rinsed.

Mast Cell Preparation and Application. The monoclonal IgE specific for DNP was labeled with Alexa 488 (Molecular Probes, Eugene, OR) according to standard procedures. RBL-2H3 cells were maintained in monolayer cultures and harvested with trypsin-EDTA (Life Technologies, Rockville, MD) 3–5 days after passage, as described previously [22] and preincubated with this anti-DNP IgE and washed as previously reported [23]. The sensitized cells were incubated with the lipid-patterned surface at 37°C for 1 hour in TYRODES buffer (in mM: 140 NaCl, 6 KCl, 1 $MgCl_2$, 2 $CaCl_2$, 10 glucose, 2 pyruvate, Aldrich, Milwaukee, WI).

Microscopy. Epifluorescence microscopy was performed with an Olympus AX 70 upright microscope, water immersion objectives, Omega Optical filter sets, and Spot CCD camera. Rhodamine and Di-I fluorescent dyes were observed with a 510-590-nm excitation/590-nm emission filter set and an Alexa 488 fluorescent dye was observed with a 450-490-nm excitation/520-nm emission filter set. SEM imaging was performed with a LEO SEM. A BioRad confocal head stage and an Olympus AX 70 inverted microscope were used for confocal

microscopy and FRAP photobleaching, the latter with a 100X objective and 10X digital zoom (100% power) for 1-minute exposures. Time series images were taken with 10-second intervals.

RESULTS

In this investigation, the aim was to create a micro- and nanometer scale array of patterned hapten-conjugated lipids for sub-cellular stimulation, test specific binding of IgE-FcεRI on sensitized RBL cells, confirm the presence of a supported lipid bilayer, investigate cell surface aggregation of IgE-FcεRI, and examine morphological changes following cellular encounter with the patterned features of squares or stripes.

An array of Di-1-POPC conjugated IgE patterns were created with sub 600-nm to 67-μm square edge widths and 0.36 μm^2 to 4,489 μm^2 surface area, respectively. The sub 600nm pattern is approximately the 500 nm threshold attainable with the 10X stepper used in this experiment. Pattern uniformity relies upon an optimized photoresist thickness of 1.5 μm and a Parylene thickness 1.0 μm, photolithography precision, optimized RIE duration to prevent underetching, and sufficient biomaterial incubation time. Application of 1 μm of Parylene and 1.5 μm of photoresist provide optimal conditions for polymer removal and patterning resolution.

Anti-DNP IgE are labeled with an Alexa-488 to monitor their binding to the DNP-conjugated lipid patterns. This binding to the DNP-conjugated lipid patterns confirms the specificity attainable with the patterned antigen target. Non-DNP-conjugated lipid bilayer surfaces demonstrate negligible fluorescence over the background fluorescence intensity. Figure 1E illustrates layering of the molecules in this patterning process. Figure 1F illustrates the structure of the DNP-conjugated POPC. The surface area of each pattern ranges from 0.283 μm^2 for the 600 nm circles to 4,489 μm^2 for the 67 μm squares. By comparison, these cells are commonly tested for 96 well plates with each well having a surface area of 44.78 mm^2!

The continuity of the supported lipid bilayer is examined with a FRAP experiment. The POPC-Di-1 lipids formed a uniform supported lipid bilayer after the five-minute incubation. A 5 μm x 5 μm patch was photobleached for one minute. The photobleaching recovers within 30-120 seconds. Supported lipid bilayer formation offers a method for creating a model cell membrane template for immobilization and stimulation. A thin film of water exists between the membrane and the substrate, as demonstrated by NMR [24] on glass beads. 100-nm vesicles appear to fuse onto silicon surfaces and form supported bilayer membranes.

RBL cells are fully immobilized on the patterned surface after one-hour incubation. The fluorescent IgE bound to FcεRI on the cell surface show the cells flattening and spreading response to stimulation. When a cell approaches a pattern edge, the cells preferentially remain in contact with the silicon substrate while still aggregating their IgE-FcεRI toward the haptenated contact interface (Figures 2A-B). When the pattern spacing is too small for a cell to squeeze between patterns, the cell rests on top of the pattern (Figure 2C). In this case, the aggregation can be observed in discrete circles around the underlying pattern. This result demonstrates that cells bind to multiple spatially separated regions on the patterned surface. In contrast, cells off the pattern remain unstimulated, rounded and not stably attached such that the majority could easily be removed in a wash step. Because the aggregated IgE-FcεRI cause coalescence of lipid rafts, there appears to be lipid raft mobility in RBL cells toward the patterned antigen.

SEM images are taken of cells immobilized and stimulated by the micro- and nanometer scale pattern. These images complement the fluorescent antibody staining images and provide clear images of the antigen stimulated, cytoskeleton-directed morphological changes. The cells extend

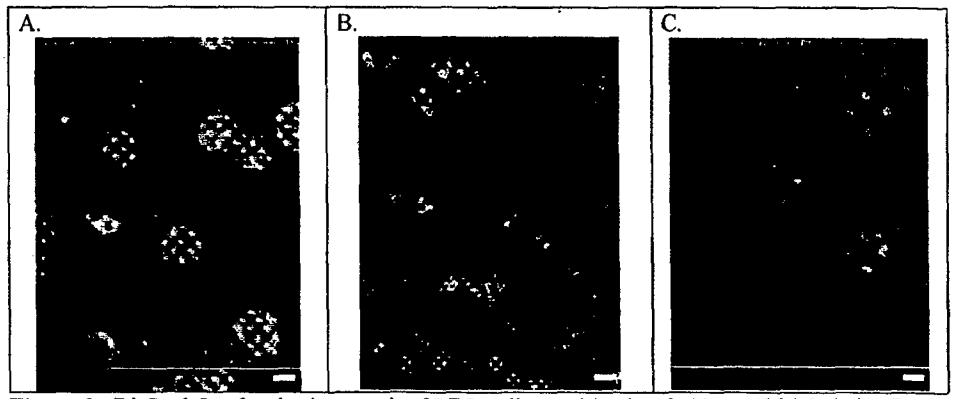

Figure 2. BioRad Confocal micrograph of RBL cells sensitized with Alexa-488 labeled IgE (green) on DNP-conjugated Di-I-DPPC patterns (red). (A) 2 μm pattern, 8 μm period, 15 μm scalebar. (B) 3-8 μm pattern, 30 μm scalebar. (C) 5 μm pattern, 15 μm period, 15 μm scalebar.

their pseudopodia along the patterned antigen forming finger-like patterns to maximize contact area (Figures 3A and 3B). Cells attempt to surround small square features (Figure 3C).

CONCLUSIONS

This procedure provides a method for analyzing cellular responses to different spatially isolated patterned antigen and controlling the antigenic surface density, the surface area covered by antigen, the spacing between features, and the actual feature dimensions. The Parylene lift-off technique offers a rapid and precise way to create supported micro- and nanometer-scale patterns of biologically active compounds. The haptenated lipid surface serves as a model of interaction of immune cells and their surroundings. The purpose of studying mast cell response is to understand localized signal transduction components, to develop a novel model system for studying cell-cell interactions such as those occurring in the immunological synapse, and to lay the groundwork for more general studies of cellular receptors and responses at interfaces.

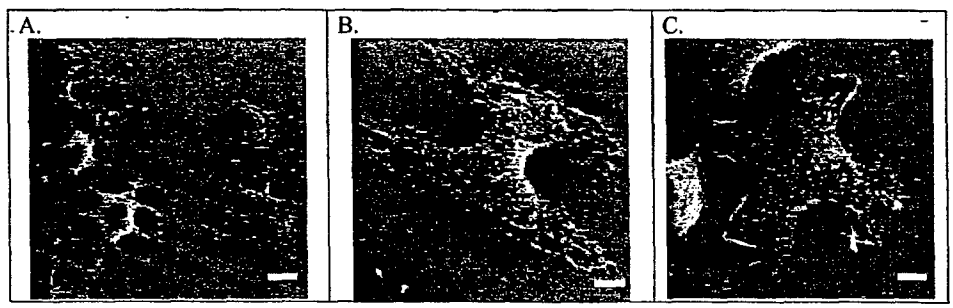

Figure 3. SEM images of stimulated RBL cells over DNP-conjugated Di-I-DPPC. (A) ~2 μm antigen lines, ~13 μm scalebar. (B) ~4 μm antigen lines, ~4 μm scalebar. (C) 4 adjacent ~4 μm antigen squares, ~4 μm scalebar.

ACKNOWLEDGEMENTS

We acknowledge the NSF support through the Nanobiotechnology Center (NBTC), an STC Program of the NSF under Agreement No. ECS-9876771, and the Cornell Nanofabrication Facility resources. We thank Mathieu Foquet for his imaging assistance, Dr. Ismail Hafez for his assistance preparing lipids, and Marisol Barrero for her manuscript review. The views expressed in this article are those of the authors and do not reflect the official policy or position of the United States Air Force, Department of Defense, or the U.S. Government.

REFERENCES

1. S. K. Bromley, W. R. Burack, K. G. Johnson, K. Somersalo, T. N. Sims, C. Sumen, M. M. Davis, A. S. Shaw, P. M. Allen, and M. L. Dustin, *Annu Rev Immunol* **19**, 375 (2001).
2. J. Medemeyer and S. J. Galli, *Br Med Bull* **56**, 936 (2000).
3. D. Holowka and B. Baird. *Sem. Immunol.* **13**, 1 (2001).
4. N. Dontha, W. B. Nowall, and W. G. Kuhr, *Anal. Chem.* **69**, 2619 (1997).
5. H. T. Tien and Z. Salamon, *Biotechnology and Applied Biochemistry* **12**, 478 (1990).
6. M. Zviman and H. T. Tien, *Biosensors & Bioelectronics* **6**, 37 (1991).
7. E. Sackman, *Science* **271**, 43 (1996).
8. R. J. Jackman, J. L. Wilbur, and G. M. Whitesides, *Science* **269**, 664 (1995).
9. C. D. James, R. C. Davis, L. Kam, H. G. Craighead, M. Isaacson, J. N. Turner, and W. Shain, *Langmuir* **14**, 741 (1998).
10. J. S. Hovis and S. G. Boxer, *Langmuir* **16**, 894 (2000).
11. L. A. Kung, L. Kam, J. S. Hovis, and S. G. Boxer, *Langmuir* **16**, 6773 (2000).
12. J. T. Groves and S. G. Boxer, *Biophysical Journal* **69**, 1972 (1995).
13. J. T. Groves, H. Ulman, and S. G. Boxer, *Science* **275**, 651 (1997).
14. P. S. Cremer, J. T. Groves, L. A. Kung, and S. G. Boxer, *Langmuir* **15**, 3893 (1999).
15. P. M. St. John, R. Davis, N. Cady, J. Czajka, C. A. Batt, and H. G. Craighead, *Anal Chem.* **70**, 1108 (1998).
16. D. V. Nicolau, T. Taguchi, H. Taniguchi, H. Tanigawa, and S. Yoshikawa, *Biosens Bioelectron* **14**, 317 (1999).
17. J. M. Corey, A. L. Brunette, M. S. Chen, J. A. Weyhenmeyer, G. J. Brewer, and B. C. Wheeler, *J Neurosci Methods* **75**, 91 (1997).
18. B. Ilic and H. G. Craighead, *Biomedical Microdevices* **2**, 317 (2000).
19. R. Orth, I. Hafez, M. Wu, B. Ilic, B. Baird, T. G. Clark and H. G. Craighead, *MRS Fall 2001 Conference Proceedings*, Section Y.7.18 (2001).
20. Avanti Polar Lipid Catalogue, Avanti Polar Lipids, Inc., Alabaster (2001).
21. L. D. Mayer, M. J. Hope, and P. R. Cullis, *Biochim Biophys. Acta.* **858**, 161 (1986).
22. L. Pierini, D. Holowka, and B. Baird. *J. Cell Biol.* 134:1427–1439 (1996).
23. D. Holowka, E. D. Sheets, and B. Baird, *J. Cell Sci.* **113**, 1009 (2000).
24. S. G. Johnson, T. M. Bayerl, D. C. McDermott, G. W. Adam, A. R. Rennie, R. K. Thomas, and E. Sachmann, *Biophys J.* **59**, 289 (1991).